Journal of The Korean Astronomical Society
32: 1 ∼ , 1999

ADAPTIVE MESH REFINEMENT IN COMPUTATIONAL ASTROPHYSICS – METHODS AND APPLICATIONS

DINSHAW BALSARA
Department of Physics, University of Notre Dame, Notre Dame, IN 46556, USA
(Received Nov 23, 2001; Accepted Nov. 26, 2001)

ABSTRACT

The advent of robust, reliable and accurate higher order Godunov schemes for many of the systems of equations of interest in computational astrophysics has made it important to understand how to solve them in multi-scale fashion. This is so because the physics associated with astrophysical phenomena evolves in multi-scale fashion and we wish to arrive at a multi-scale simulational capability to represent the physics. Because astrophysical systems have magnetic fields, multi-scale magnetohydrodynamics (MHD) is of especial interest. In this paper we first discuss general issues in adaptive mesh refinement (AMR). We then focus on the important issues in carrying out divergence-free AMR-MHD and catalogue the progress we have made in that area. We show that AMR methods lend themselves to easy parallelization. We then discuss applications of the RIEMANN framework for AMR-MHD to problems in computational astophysics.

Key Words : methods: numerical – AMR – MHD – ISM: supernovae – magnetic fields – Star Formation: collapse – fragmentation – protostars

I. INTRODUCTION

Observations of various astrophysical systems such as proto-stars, novae, supernovae, the interstellar medium, galaxies and cosmology show that physical processes in these systems evolve in multi-scale fashion. To take but a single example from proto-star formation, once a Class 0 core forms out of the turbulent, magnetized, molecular gas in a molecular cloud, gravity causes the system to be largely decoupled from the rest of the turbulent flow. And yet, the decoupling is not complete. Large-scale magnetic fields cause the proto-star's angular momentum to be coupled to that of the external medium. Likewise, different parts of the dusty protostellar envelope are radiatively coupled to each other. The radiative coupling also sets the temperature of the gas, thereby determining its coupling with the magnetic field. As a result, we see the need for: (1) detailed representation of the micro-physical processes, (2) accurate representation of the system of equations that are of interest in computational astrophysics and (3) an ability to do (1) and (2) in a multi-scale fashion via adaptive mesh refinement (AMR). AMR is an elegant technique for concentrating mesh resolution in regions where an accurate answer is desired. Almost all astrophysical processes have magnetic fields and so an ability to represent MHD in multi-scale fashion is a *sine qua non* for computational astrophysics. The present paper focusses on recent advances by the author that have made it possible to carry out AMR-MHD calculations.

Ever since the first paper on AMR methods for fluid dynamics, see Berger and Colella (1989), it has been recognized that that higher order Godunov schemes play a central role in practical AMR simulations. The reasons are not difficult to see and the talks by Ryu (this conf.) on MHD, Ibanez and Koide (again this conf.) on relativistic flow bear testimony to the usefulness of these techniques in computational astrophysics. Such schemes were first formulated for hydrodynamics by vanLeer (1979), where their usefulness has been very well-documented by Woodward and Colella (1984). In recent years, they have been formulated for several other systems of interest in computational astrophysics wich include relativistic hydrodynamics, see Balsara (1994); radiation hydrodynamics, see Balsara (1999a,b,c); radiation MHD, see Balsara (1999d,e); relativistic MHD, see Balsara (2001a) and multidimensional radiative transfer, see Balsara (2001b). Perhaps the most vigorous evolution has taken place in MHD where Roe and Balsara (1996) designed the first complete MHD eigenvectors that were free of singularities; Brio and Wu (1988), Zachary, Malagoli and Colella (1994), Powell (1994), Dai and Woodward (1994), Ryu and Jones (1995) and Balsara (1998a) designed Riemann solvers for MHD; Dai and Woodward (1995), Ryu et al (1998) and Balsara (1998b) catalogued different forms of TVD schemes for MHD and Balsara and Spicer (1999), Dai and Woodward (1998), Ryu et al (1998), Londrillo and Del Zanna (2000) and Toth (2000) formulated divergence-free higher order Godunov schemes for MHD. The latter divergence-free formulations realize that the divergence of the magnetic field should remain exactly zero. Brackbill and Barnes (1980) and Brackbill (1985) have shown that violating the constraint leads to unphysical plasma transport orthogonal to the magnetic field as well as a loss of momentum and energy conservation. Powell et al (1999) did indeed formulate an AMR scheme for MHD that was not divergence-free only to find that the maximal errors ocurred on the finest meshes due to unphysical build-up of divergence. The finest meshes are the very

meshes where one would have wanted the error to be minimal! Moreover, in accreting astrophysical flows, the divergence would flow with the fluid and build up in the very regions where one wants the most accurate answer! This prompted the present author to realize that only a scheme that was divergence-free on the entire AMR hierarchy would be adequate for astrophysical applications. These advances have been catalogued in detail in Balsara (2001c) and implemented in the RIEMANN framework for computational astrophysics. While Balsara (2001c) provides more mathematical details, the present paper focusses more on the intuitive ways of thinking about the subject. As a result, the two papers complement each other.

In Section II we discuss algorithmic issues in AMR hydrodynamics. In Section III we discuss divergence-free AMR-MHD. In Section IV we show how AMR-MHD techniques have been parallelized. In Section V we discuss tests and applications.

II. AMR HYDRODYNAMICS

Fig. 1 provides a schematic of a two-dimensional AMR calculation where we show a large mesh zone and an adaptively refined set of four finer mesh zones adjacent to it. The large mesh zone should be viewed as being part of a coarse mesh and the four finer mesh zones should be viewed as being part of a fine mesh in the AMR hierarchy that abuts the above-mentioned coarse mesh. A consideration of that figure allows us to motivate the four most important algorithmic issues in AMR-hydrodynamics that were formulated by Berger and Colella (1989) (hereafter BC). They are:

(II.a) Time step sub-cycling on refined meshes: A look at Fig. 1 shows that the finer mesh has zones that are half as small as the coarse mesh. As a result, the Courant condition for time step control decrees that the finer mesh can only evolve with time steps that are half as small as the coarse mesh time steps. This is illustrated in the schematic time-axis in Fig. 1. As a result of this limitation, BC realized that the fine mesh should move with a time step that is an integral fraction of the coarse mesh time step. The precise fraction is determined by the mesh refinement ratio. As a result, the fine mesh will undergo more than one time steps before it reaches time-synchonization with the coarse mesh.

(II.b) Prolongation of coarse mesh solution to fine mesh boundaries/or new fine mesh interiors: As the fine mesh undergoes fractional time steps, it will receive temporally interpolated boundary information from the abutting coarse mesh. Even when a new fine mesh is built in a portion of the coarse mesh that was not covered by a fine mesh, one has to find a *conservative* strategy for transferring the solution from the coarse mesh to the fine mesh. This step is known as prolongation. To prolong the solution from the coarse mesh to the fine mesh one has to use the conservative interpolation of the underlying higher order Godunov scheme.

(II.c) Flux correction at the fine-coarse interface: When the fine mesh and coarse mesh solutions are synchronized, we want to ensure conservation of mass, momentum and energy. As pointed out by BC, a failure to ensure full conservation will result in spurious solutions on the entire AMR hierarchy. This is especially true for most astrophysical systems which give rise to very deep AMR hierarchies, thereby exacerbating the problems associated with a loss of conservation. This ability to ensure conservation is only available when using a higher order Godunov scheme as the underlying solution technique. For example, the staggered mesh formulation of the ZEUS scheme of Stone and Norman (1991) cannot ensure conservation of all variables on AMR hierarchies, thereby limiting its utility for AMR simulations. The flux conservation can be imposed at the times when the fine and coarse meshes are synchronized. This happens at times t^n and t^{n+1} where the time step is given by $\Delta t = t^{n+1} - t^n$. The flux conservation is carried out by replacing the coarse mesh flux $F^{n+1/2}_{i+1/2,j}$ by a spatial and temporal average of the fine mesh fluxes, i.e. $f^{n+1/4}_{m-1/2,p}$, $f^{n+1/4}_{m-1/2,p+1}$, $f^{n+3/4}_{m-1/2,p}$ and $f^{n+3/4}_{m-1/2,p+1}$, at the interface between the fine and coarse mesh as shown in Fig. 1. As a result, a layer of coarse mesh zones that abut the fine mesh zones will have to undergo this flux correction. The variable $U^{n+1}_{i,j}$ will, therefore, undergo flux-correction, as shown in Fig. 1, whenever the fine and coarse meshes synchronize in time.

(II.d) Restriction of fine mesh solution to coarse mesh: When the fine and coarse meshes are time synchronized, the fine mesh holds the more accurate solution. As a result, we replace the coarse mesh solution by the spatially averaged fine mesh solution. This step is known as restriction.

This completes the process of demonstrating the four essential steps in BC's AMR strategy for hydrodynamics. These four steps yield a scheme that is fully *conservative* of mass, momentum and energy. Notice that the coarse meshes deliver their data to the fine mesh in step (b) above. Likewise, the fine meshes deliver data that is generated on them to modify the coarse mesh data in steps (c) and (d). As a result, the solution that evolves on an AMR hierarchy is intimately connected across the levels in the AMR hierarchy! This ensures that all the levels in the AMR hierarchy are causally connected. It also ensures that a spurious solution generated on one level in an AMR hierarchy (for example, the finest level in the scheme of Powell et al (1999)) will eventually propagate and corrupt the solution at all levels in the AMR hierarchy. This brings out the very interesting fact that AMR techniques are physically consistent at a very deep level. At the same time, it shows that violating that consistency can result in a solution that is flawed at all levels (all puns intended!).

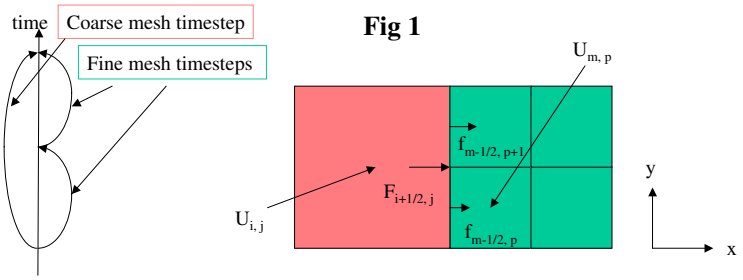

$$U_{i,j}^{n+1}=U_{i,j}^{n+1}-\frac{\Delta t}{\Delta x}\left[\frac{1}{4}\left(f_{m-1/2,p}^{n+3/4}+f_{m-1/2,p+1}^{n+3/4}+f_{m-1/2,p}^{n+1/4}+f_{m-1/2,p+1}^{n+1/4}\right)-F_{i+1/2,j}^{n+1/2}\right]$$

Spatial and temporal average of fine mesh fluxes

$$B_{z;\,i,j}^{n+1}=B_{z;\,i,j}^{n+1}-\frac{\Delta t}{\Delta x}\left[\frac{1}{4}\left(e_{y;\,m-1/2,p}^{n+1/4}+e_{y;\,m-1/2,p+1}^{n+1/4}+e_{y;\,m-1/2,p}^{n+3/4}+e_{y;\,m-1/2,p+1}^{n+3/4}\right)-E_{y;\,i+1/2,j}^{n+1/2}\right]$$

Spatial and temporal average of fine mesh electric fields

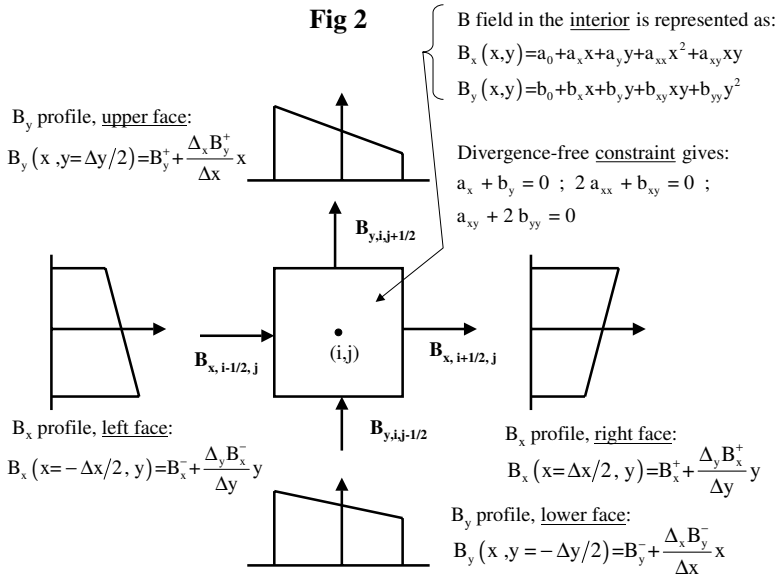

III. DIVERGENCE-FREE AMR-MHD

The previous section suggests that it would be desirable to have a similar strategy for AMR-MHD. However, a little thought reveals a major obstacle. We saw in section II.b that it was essential to use the reconstruction strategy for the underlying higher order Godunov scheme in order to arrive at a conservative strategy for AMR-hydrodynamics. However, up until recently, an analogous divergence-free reconstruction strategy for (divergence-free) magnetic fields did not exist. As a result, it was not possible to formulate divergence-free AMR-MHD because it was not possible to transfer the magnetic fields in divergence-free fashion from a coarse mesh to a fine mesh. In retrospect this lack of a divergence-free reconstruction strategy might seem a little surprising since the formulation of a reconstruction strategy is central to the process of designing a higher order Godunov scheme. Balsara and Spicer (1999) had, nevertheless, been able to design a second order accurate Godunov scheme for divergence-free MHD without having to address the reconstruction question. The reason one is able to bypass the issue of divergence-free reconstruction in the formulation of second order Godunov schemes stems essentially from a mathematical anomaly. It turns out that for second order schemes (and only for second order schemes) it is possible to get by without having to address the issue of divergence-free reconstruction. However, in order to formulate a divergence-free AMR-MHD one has to face up to the the task of formulating a divergence-free reconstruction strategy. We do that next for two-dimensions in this paper. Mathematical details associated with the two-dimensional case as well as the analogous three-dimensional problem are catalogued in Balsara (2001c).

Consider Fig. 2 which shows the four magnetic field components on the four faces of a square. This is the lay-out of magnetic field variables from Balsara and Spicer (1999) and yields a scheme for divergence-free magnetic field evolution. To arrive at a second order accurate formulation we endow the field components with piecewise linear variation in the transverse direction as shown in Fig. 2. One may well wonder why this should necessarily yield a second order accurate formulation. It can be shown, see Balsara (2001c), that for variations that are restricted to lie in one dimension, this yields a second order accurate TVD scheme. Multidimensional TVD schemes can be build out of such one dimensional building blocks. As a result, we know that the strategy of endowing the field components with piecewise linear variations in the transverse direction will yield a second order accurate representation of the field in the interior of the square. The most general polynomial representation of the vector field in the interior of the square that matches the linear profiles at the boundaries is also given in Fig. 2. In order for the polynomials to be divergence-free the polynomial coefficients should satisfy the divergence-free constraints, also given in Fig. 2. These constraints can be straightforwardly derived by taking the divergence of the polynomials. The result is that the independent polynomial coefficients are exactly specified by specifying the piecewise linear variation of the field components in the transverse direction. A similar result obtains in three dimensions. We are now in a position to specify the magnetic field at any point in the interior of the square – this being the problem of divergence-free reconstruction. It is now easy to see that if the square is subdivided into four squares through the refinement process we can still specify the magnetic field at the faces of each of the four smaller squares. Because the generating polynomial is divergence-free, this specification is also divergence-free. This solves the problem of divergence-free prolongation from coarse meshes to fine meshes. It is now easy to specify the four important algorithmic issues in divergence-free AMR-MHD. They are:

(III.a) Time step sub-cycling on refined meshes: This is entirely analogous to section II.a.

(III.b) Divergence-free prolongation of coarse mesh magnetic field to fine mesh boundaries: This is discussed in the two paragraphs above. For three dimensions the problem becomes more complicated but it has been worked out in detail by Balsara (2001c).

(III.c) Electric field correction at the fine-coarse interface: In section II.c we saw that whenever the fine and coarse meshes are time-synchronized the fine and coarse mesh fluxes have to be made consistent at the interface between the fine and coarse mesh. The electric field plays a central role in the divergence-free evolution of the magnetic field, just as the flux plays a central role in the evolution of higher order Godunov schemes. As a result, following a style of reasoning that is entirely analogous to section II.c, we have to make the electric field consistent at the interface. This is illustrated in Fig 1 for the evolution of the z-component of the magnetic field. Further details have been provided in Balsara (2001c).

(III.d) Restriction of fine mesh solution to coarse mesh: In a direct analogy to Section II.d, when the fine and coarse meshes are temporally synchronized we replace the coarse mesh magnetic fields by the area-averaged fine mesh magnetic fields.

IV. PARALLEL PROCESSING OF AMR HIERARCHIES

The previous two sections have described the algorithmic issues in divergence-free AMR-MHD in some detail. However, carrying out an AMR calculation requires one to understand several further issues. They can be illustrated by looking at Fig. 3 which shows an AMR-MHD simulation of a supernova remnant. Figs. 3a and 3b show the log of the density and pressure variables. Figs. 3c and 3d show the Mach number and the magnitude of the magnetic field. Fig. 3e shows the color coded levels in the AMR hierarchy, blue being the base level grid, yellow being the first level of refinement and red being the second level of refinement. Fig. 3f shows the divergence of the magnetic field showing that it remains within the bounds of machine accuracy. This allows us to motivate several issues in supporting parallel AMR calculations, all of which are catalogued in detail in Balsara and Norton (2001). The issues are:

(IV.a) Object-oriented representation of the AMR hierarchy: We see from Fig. 3e that the meshes concentrate themselves in regions of strong shock, which is what we desire from an AMR calculation. However, We see that each level of refinement is made of many small meshes, all of which taken together form the AMR level. This requires a high level of abstraction modeling so that each small mesh, along with all the data structures that are needed for representing the MHD solver on a mesh can be manipulated as a single unit. This is made possible by object-oriented methods which allow us to encapsulate the data as well as the functions that change the data as a single unit.

(IV.b) Load balancing of each level: AMR computations are CPU and memory intensive. As a result, it is important to carry them out on parallel machines. However, it is difficult to know how to deal out the different meshes to the different processors of a parallel machine. This process of dealing the meshes out should be done in such a way that each processor should has the same amount of computational load. This is done via a load balancer. Several different load balancer strategies are catalogued and inter-compared in Balsara and Norton (2001).

(IV.c) Parallel processing of the AMR hierarchy: Parallel processing of the AMR hierarchy is tantamount to processing each level in the AMR hier-

archy in a load balanced fashion. Balsara and Norton (2001) have shown that this can be done using modern parallel processing techniques along with the load balancer described above.

(IV.d) Solution-adaptive evolution of the AMR mesh hierarchy: We see that as the SNR shock moves through the mesh, the grids that make up the levels have to change in response to the shock. This requires that one is able to flag regions that need refinement and put down new refined meshes where they are called for while removing old refined meshes from regions that do not require refinement any longer. Such strategies were developed by Berger and Rigoutsis (1991) and Balsara and Norton (2001) have shown that they are easily parallelized.

V. TESTS and APPLICATIONS

(V.a) Test of Supernova Remnant Explosion: Balsara (2001c) provides several test problems to demonstrate divergence-free AMR-MHD. The present test problem is motivated by the work of Balsara, Benjamin and Cox (2001) (hereafter BBC) who simulated the evolution of supernova remnants and their propagation through the magnetized interstellar medium (ISM) on large, i.e. 256^3 zone, meshes. In this test problem we do one of the same problems from BBC using AMR-MHD on a 64^3 zone base mesh and two levels of refinement. Since the mesh refinement was carried out with a refinement ratio of two across each level, the simulation with AMR has the same effective resolution as the large uniform mesh simulation. Fig 3 shows the variables from the AMR-MHD simulation. In Section IV we catalogued the variables that were plotted out in each of the sub-figures in Fig. 3. Similar variables from the large uniform mesh simulation have been shown in BBC. It can be seen that for the same effective resolution, the AMR-MHD simulation produces the same quality of solution as the simulation presented in BBC. This shows that there are some systems in computational astrophysics where it is possible to intercompare the AMR-MHD simulation with a large uniform mesh simulation and verify that the two simulations produce the same quality of result if they have the same effective resolution. This is a powerful demonstration of the saliency and effectiveness of AMR-MHD techniques in computational astrophysics. We also notice from Fig. 3f that the divergence of the magnetic field has remained within the bounds of machine accuracy!

(V.b) Application to Protostellar Core Collapse and Fragmentation: Understanding how protostellar cores form from a rotating density condensation has long been a problem of great interest in star formation studies. However, previous studies, see Truelove et al (1997) and Boss et al (2000) have been hydrodynamical. The above authors have shown that AMR is extremely useful for such simulations because the formation of density condensations is not correctly represented when the mesh-based Jeans criterion is not met (which inevitably happens in a uniform mesh calculation). I.e. if too much mass is concentrated in one zone so that the zone becomes Jeans unstable then the fluid flow is not properly represented on such a mesh. In such situations, our only recourse is to refine the mesh. The above-mentioned hydrodynamical studies permit one to answer some questions. However, they do not permit one to answer the important questions associated with the inclusion of magnetic fields: (1) How does the inclusion of magnetic fields change the disks that form? (2) Does the magnetic field naturally form an hourglass morphology? (3) How does the angular momentum evolve? (4) Do outflows form? Can we understand their formation mechanism? (5) The inclusion of fields introduces a competition between three timescales – the free-fall timescale, the magnetic braking timescale and the ambipolar diffusion timescale. How do those three timescales compete with each other?

Fig. 4 from Balsara and Burkert (2001) shows figures from an AMR-MHD simulation of this problem on a 128^3 zone base mesh with four further levels of refinement. The magnetic field was aligned with the rotation axis which was taken to be the z-axis. The barotropic approximation of Boss et al (2000) was used but ambipolar diffusion was not included. Fig. 4a shows the log (density) in the xy-midplane at a relatively early time. We see that the system fragments into two disks, just like in the hydrodynamical case. Fig. 4b shows the same variable at a late time. We now see that the disks in the MHD simulation have lost angular momentum and coalesced, unlike the hydrodynamical case. This can be explained via mechanisms similar to the magnetic braking idea of Paleologou and Mouschovias (1983). Fig. 4c shows the magnetic field in the xy-plane at the same time as Fig. 4b demonstrating that the field has been dredged in by the infall. The field, however, is connected to the ambient gas and so imparts some of the two-disk system's angular momentum to the ambient gas. The ambient medium is thus spun up at the expense of the two-disk system which eventually inspirals and coalesces to form a single disk as shown in Fig. 4b. Fig. 4d shows a color coded representation of the levels at the same time as Figs. 4b and 4c showing how the levels are nested one within the other and how they track the increasing density. Fig. 4e shows a zoomed view of the magnetic field lines in the central part of the yz-midplane at a late time. We see that the accretion processes have caused the field to naturally organize itself into an hourglass morphology. The colors in Fig. 4e track magnetic pressure. Fig. 4f shows the z-velocity in the same portion of the yz-midplane. We see from the colors that an outflow has been established. We claim that it is a magneto-centrifugal outflow because it establishes itself in the same areas of the rotating gas where the gas has a substantial rotational velocity and is restricted to regions where the magnetic field makes a large angle with the rotation axis. This is consistent with the theory for MHD-outflows presented

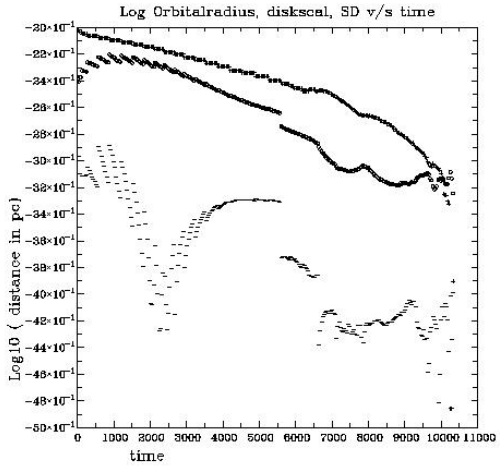

Fig 5a

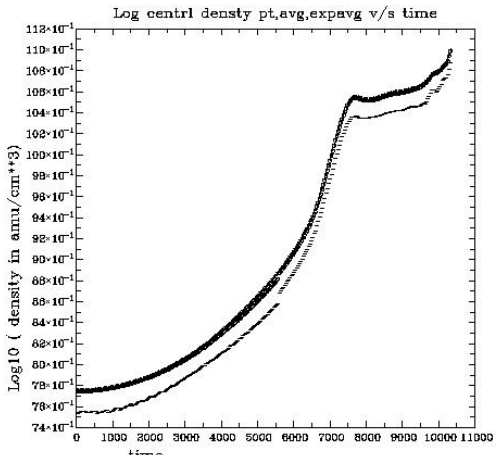

Fig 5b

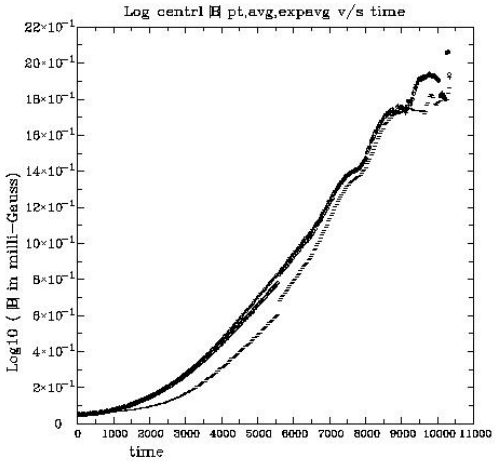

Fig 5c

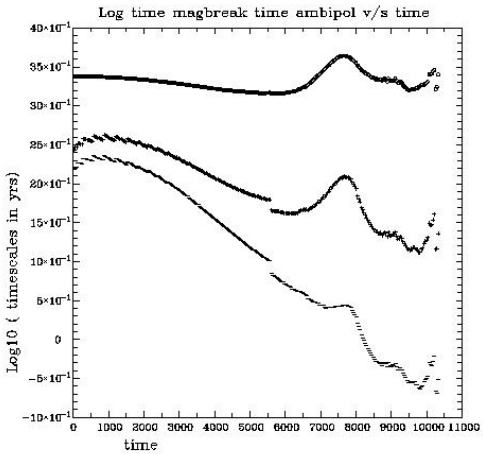

Fig 5d

by Blandford and Payne (1982).

In Fig. 5 we show plots that make several aspects of the problem more quantitative. Bacmann et al (2001) found that Class 0 cores have a centrally flattened density profile. In keeping with their observation, we fit the profiles of either disk to a Gaussian profile $\rho \sim exp[-(R/R_D)^2]$ where R is the radius of the disk and R_D is the scale of the disk. The top curve in Fig. 5a shows the distance between the disks (in pc) as a function of time (in years). The middle curve in Fig. 5a shows R_D as a function of time. We see that at $\sim 7500yrs$ the disks coalesce resulting in a cusp in either of the two curves. The lower (and very jagged) curve in Fig. 5a traces out the standard deviation in our measurement of R_D . We see that the standard deviation is substantially smaller than our measurement of R_D , indicating that our choice of a Gaussian density profile was a good one. (We note, however, that the observations and simulations have latitude for other centrally flattened profile fits. However, any centrally flattened profile would make allowance for a flattening length scale much like R_D .) It is worthwhile asking how the central density and magnetic field in the disks evolve? The upper plots in Figs. 5b and 5c show the evolution of the central density and magnetic pressure respectively in the disk/s as a function of time. The lower plots in Figs. 5b and 5c measure the mean density and magnetic field in the disk/s averaged over the disk scale R_D . Again, the reorganization of material at the time of coalescence at $\sim 7500yrs$ is shown by a cusp in either plot. While the central density can reorganize itself the central field cannot. As a result, the field shows a steeper rise than the density after $\sim 7500yrs$. It is always worthwhile asking how the inclusion of ambipolar drift (AD) would change this scenario. Should AD operate, this process of dredging in field would not be as pronounced. While we have not included AD, we have evaluated its effect on a post-facto basis. This is important because the the free-fall, the magnetic braking and AD timescales compete in regulating the early evolution of protostellar cores. This is shown in Fig. 5d where the upper plot shows the magnetic braking time, the middle plot shows the ambipolar diffusion time for cosmic ray heating and the lower plot shows the ambipolar diffusion time for far ultraviolet heating. The infall time is a little larger than the magnetic braking time. We see that the braking does dominate in this problem so that the disks coalesce before infall

to the center, as would be expected in such a situation. However, with the inclusion of AD, it is possible for the AD timescales to be much shorter suggesting that AD could reorganize the field structures in times that are shorter than the infall time. To summarize, the inclusion of magnetic fields has indeed shown the rich interplay of new physics and timescales in this very important problem.

VI. CONCLUSIONS

Several advances in divergence-free AMR-MHD and its application to astrophysics are reported here. We list them below:

(1) A general strategy is presented for the time-update of the MHD system of equations on AMR hierarchies.

(2) Just as Berger and Colella (1989) reduced the conservative time-update of the Euler equations on an AMR hierarchy to the application of a few simple steps, we have reduced the divergence-free time-update of the MHD equations on an AMR hierarchy to the application of a few simple steps. The steps have been summarized in Section III.

(3) A significant advance has been made in the divergence-free reconstruction of vector fields.

(4) Divergence-free prolongation of magnetic fields on an AMR hierarchy can be carried out via a very slight extension of the divergence-free reconstruction scheme mentioned in the previous point.

(5) A divergence-free restriction strategy is presented.

(6) An electric field correction strategy is presented which restores the consistency of electric fields at a fine-coarse interface in the AMR hierarchy.

(7) Because of the above four points, the time-step can be sub-cycled on finer meshes without loss of the divergence-free property of the magnetic fields.

(8) The above-mentioned innovations have been incorporated in the RIEMANN framework for parallel, self-adaptive computational astrophysics. Several stringent test problems have been presented and it is shown that the method presented in this paper for AMR-MHD is truly divergence-free.

(9) Several very useful insights into astrophysical processes have been derived from the AMR-MHD simulations that have been presented.

ACKNOWLEDGEMENTS

This work was supported by NSF grants AST-0132246 and 005569-001.

REFERENCES

Bacmann, A. et al, A & A, to appear (2001)

Balsara, D.S., J. Comput. Phys., vol. 114, 284, (1994)

Balsara, D.S., Ap.J.Supp., vol. 116, pg. 119, (1998a)

Balsara, D.S., Ap.J.Supp., vol. 116, pg. 133, (1998b)

Balsara, D.S., JQSRT, vol 61(5), 617, (1999a)

Balsara, D.S., JQSRT, vol 61(5), 629, (1999b)

Balsara, D.S., JQSRT, vol 62, 167, (1999c)

Balsara, D.S., JQSRT, vol 61 (5), 637, (1999d)

Balsara,D.S., JQSRT, vol 62, 167, (1999e)

Balsara, D.S. and Spicer, D.S., J. Comput. Phys., vol. 149, pg. 270, (1999)

Balsara, D.S., vol. 132, pg. 1, Astrophys.J.Supp., (2001a)

Balsara,D.S., JQSRT, vol 69(6), 671, (2001b)

Balsara, D.S., to appear, J. Comput. Phys., (2001c)

Balsara, D.S., and Norton, C.D., Parallel Computing, vol. 27, pgs. 37-70, (2001)

Balsara, D.S., Benjamin, R. and Cox, D., "The Evolution of Adiabatic Supernova Remnants in a Turbulent Magnetized Medium", 2001, to appear, Astrophys. J., vol. 563

Balsara, D.S. and Burkert, A., "Three Dimensional AMR-MHD Simulations of Protostellar Core Collapse and Fragmentation", 198^{th} AAS Conf.

Berger,M., and Colella,P., J. Comput. Phys., vol. 82, pp. 64, (1989)

Berger,M., and Rigoutsos, I., IEEE Transactions on System, Man and Cybernetics, vol. 21, pp. 61-75, (1991)

Blandford, R.D. and Payne, D.G., MNRAS, 199, 883, (1984)

Boss, A.P., et al, Ap.J., 528, 325, (2000)

Brackbill, J.U., and Barnes, D.C., J. Comput. Phys., vol. 35, pg. 462 (1980)

Brackbill, J., Space Sci. Rev., vol. 42, pg. 153 (1985)

Brio, M. and Wu, C.C., J. Comput. Phys., v75, pp. 400-422, (1988)

Dai, W., and Woodward, P.R., J. Comput. Phys., vol. 111, pg. 354, (1994)

Dai, W., and Woodward, P.R., Astrophys. J., vol. 494, pg. 317, (1998)

Londrillo, P., and Del Zanna, L., Astrophys. J., vol. 530, pg. 508, (2000)

Paleologou, M. and Mouschovias, T.C., Ap.J., 275, 838, (1983)

Powell, K.G., ICASE Report No. 94-24, Langley VA, (1994)

Powell, K.G., Roe,P.L., Linde, T.J., Gombosi, T.I., and DeZeeuw, D.L., J. Comput. Phys., vol. 154, pg. 284, (1999)

Roe,P.L., and Balsara, D.S., SIAM J. Num. Anal., 56, 57, (1996)

Ryu,D., and Jones,T., Ap. J., 442, 228, (1995)

Ryu, D., Miniati, F., Jones, T.W., and Frank, A., Astrophys. J., vol. 509, pg. 244, (1998)

Truelove, J.K. et al, Ap.J., 489, 179, (1997)

VanLeer, B., J. Comput. Phys., v32, pp.101-136, (1979)

Woodward, P., and Colella, P., J. Comput. Phys., v54, pp. 115-173, (1984)

Zachary, A.L., Malagoli, A., and Colella, P., SIAM J. Sci. Comput., vol. 15, pg. 263, (1994)

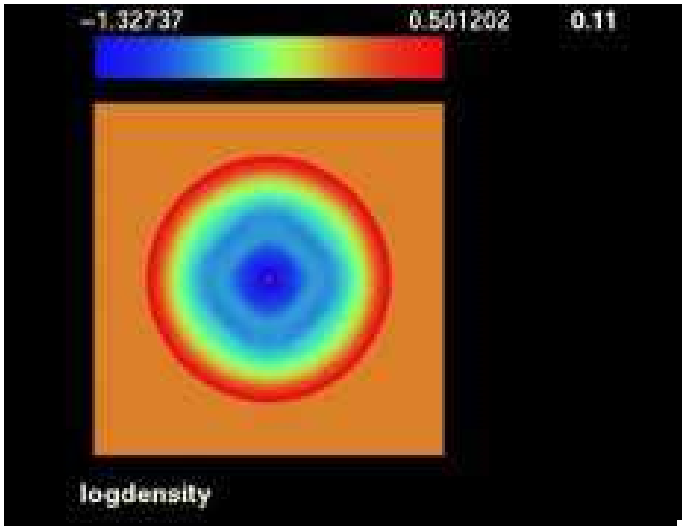

Fig 3a

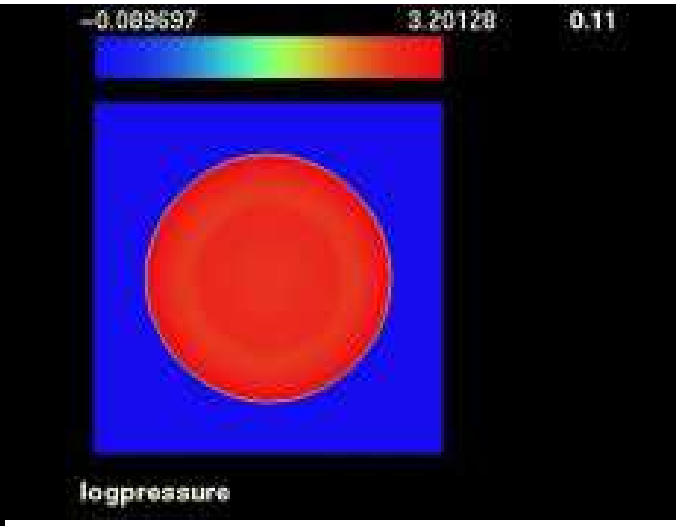

Fig 3b

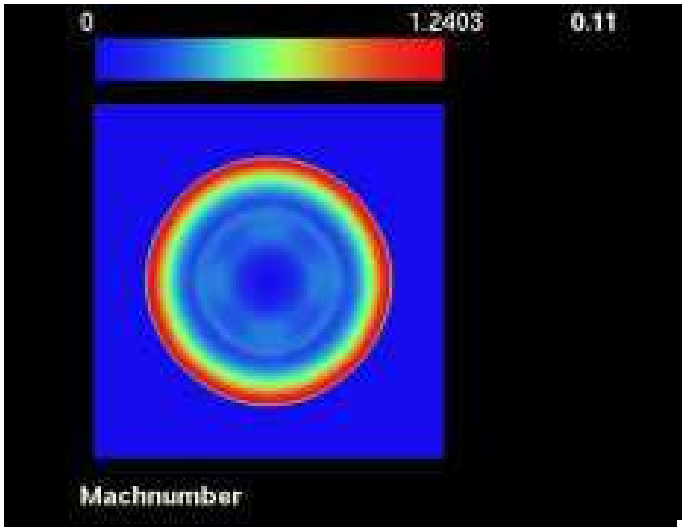

Fig 3c

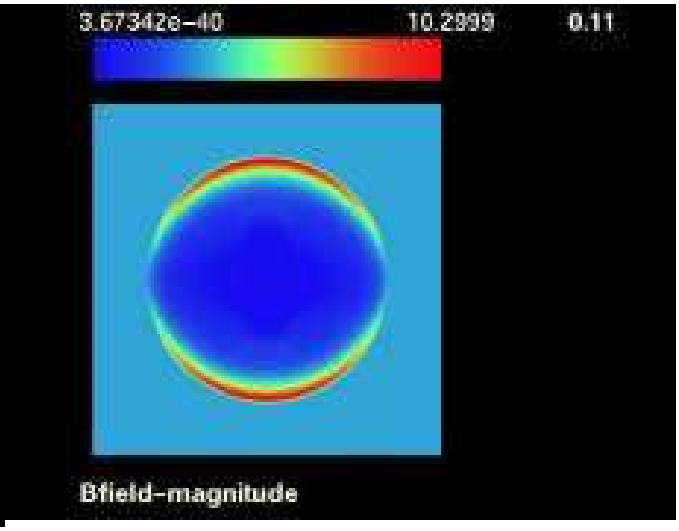

Fig 3d

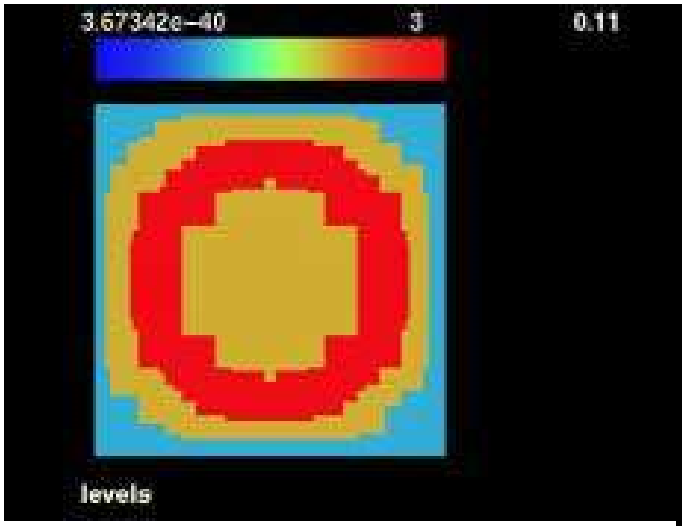

Fig 3e

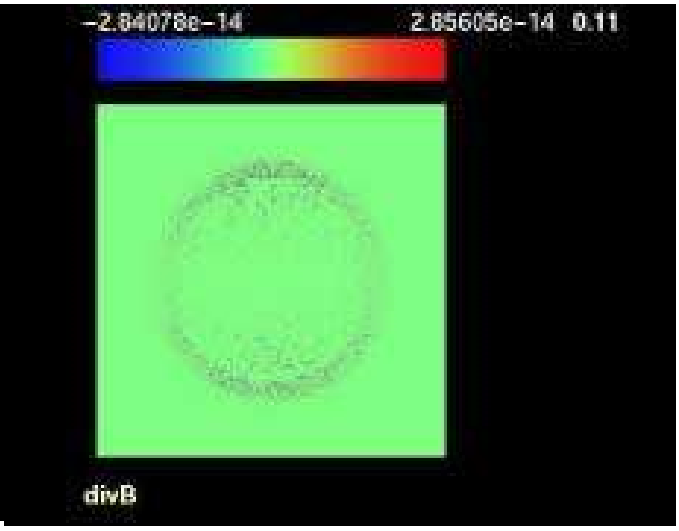

Fig 3f

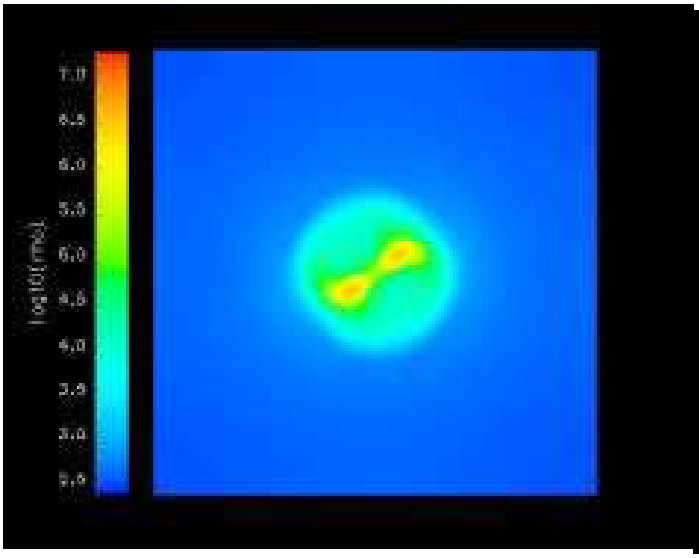

Fig 4a

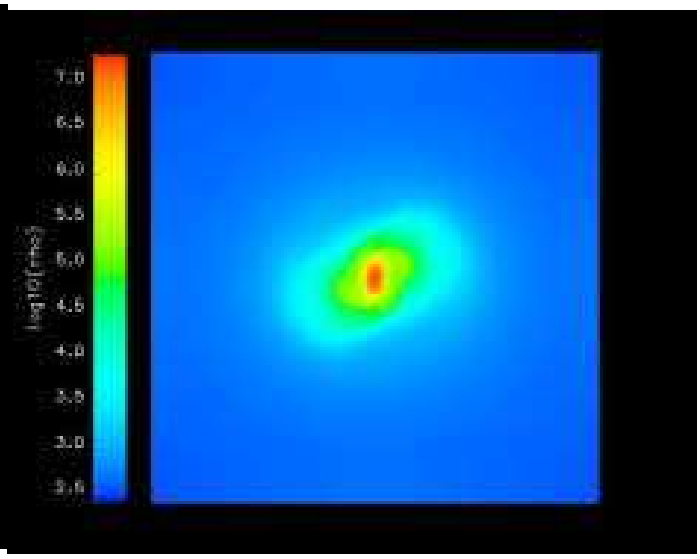

Fig 4b

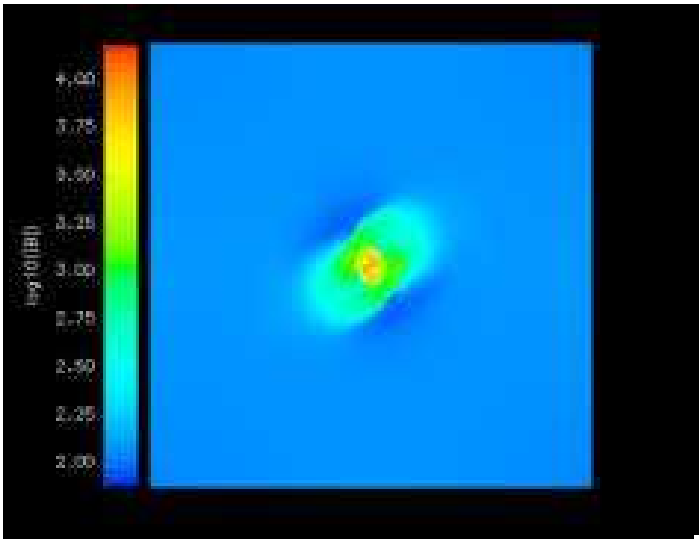

Fig 4c

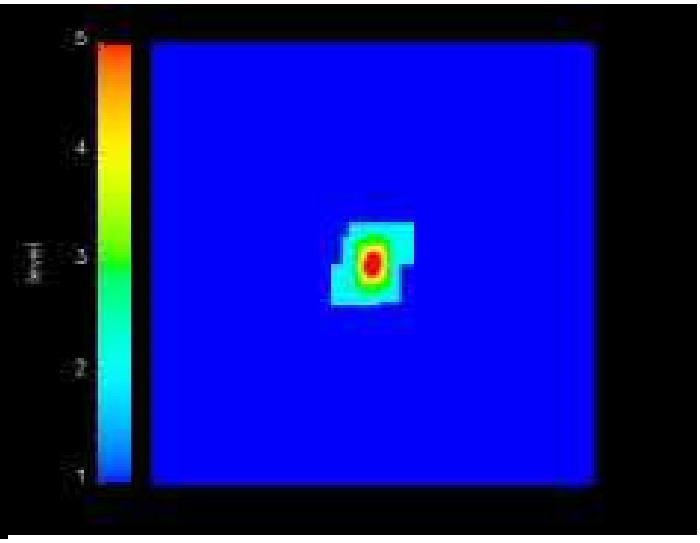

Fig 4d

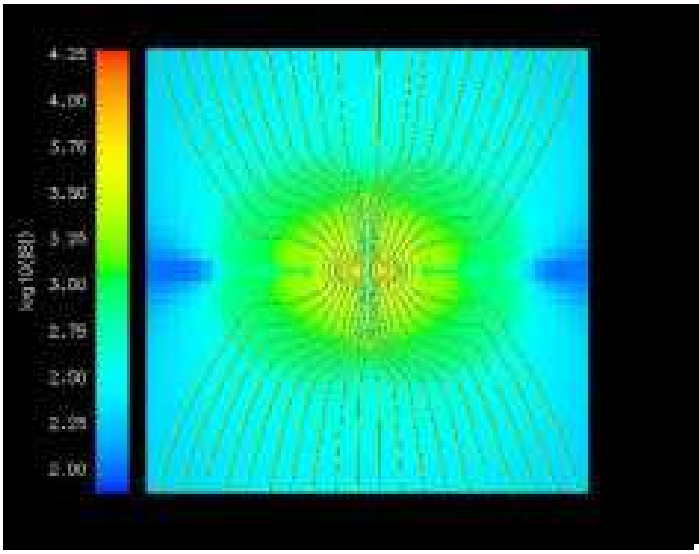

Fig 4e

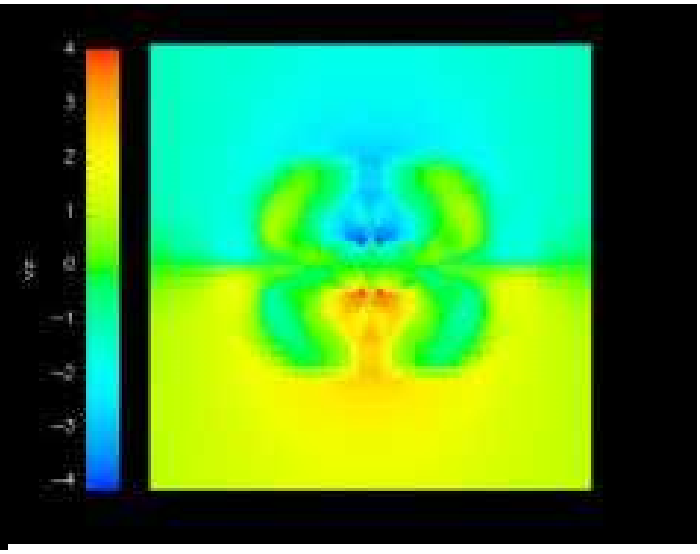

Fig 4f